Computers and Concrete, *Vol. 25, No. 4 (2020) 327-341*
DOI: https://doi.org/10.12989/cac.2020.25.4.327

Development of a user-friendly and transparent non-linear analysis program for RC walls

Scott J. Menegon*[1], John L. Wilson[1], Nelson T.K. Lam[2] and Emad F. Gad[1]

[1]*Department of Civil and Construction Engineering, Swinburne University of Technology, John Street Hawthorn VIC 3122, Australia*
[2]*Department of Infrastructure Engineering, University of Melbourne, Parkville VIC 3010, Australia*

(*Received September 3, 2019, Revised March 22, 2020, Accepted March 23, 2020*)

Abstract. Advanced forms of structural design (e.g., displacement-based methods) require knowledge of the non-linear force-displacement behavior of both the overall building and individual lateral load resisting elements, i.e., walls or building cores. Similarly, understanding the non-linear behaviour of the elements in a structure can also allow for a less conservative structural response to be calculated by better understanding the cracked (i.e., effective) properties of the various RC elements. Calculating the non-linear response of an RC section typically involves using 'black box' analysis packages, wherein the user may not be in complete control nor be aware of all the intricate settings and/or decisions behind the scenes. This paper introduces a user-friendly and transparent analysis program for predicting the back-bone force displacement behavior of slender (i.e., flexure controlled) RC walls, building cores or columns. The program has been validated and benchmarked theoretically against both commonly available and widely used analysis packages and experimentally against a database of 16 large-scale RC wall test specimens. The program, which is called WHAM, is written using Microsoft Excel spreadsheets to promote transparency and allow users to further develop or modify to suit individual requirements. The program is available free-of-charge and is intended to be used as an educational tool for structural designers, researchers or students.

Keywords: RC walls; reinforced concrete walls; non-linear analysis of RC walls

1. Introduction

Advanced forms of structural analysis for reinforced concrete (RC) buildings or bridges, such as displacement-based seismic design procedures, require the designer to calculate or have some knowledge of the non-linear force-displacement behaviour of the individual RC elements (e.g., walls or columns), or the structure as a whole. Designers typically rely on commercially available 'black box' analysis packages to calculate the non-linear response of an RC section. The primary objective of this study is to develop an alternative non-linear analysis package for predicting the back-bone force-displacement behavior of RC walls and building cores that was both transparent and simple-to-use. This resulted in a program that was developed and written using Microsoft Excel spreadsheets. The program is called WHAM and is available free-of-charge. The program can be downloaded from Menegon (2019) or by contacting the corresponding author.

During development there was an emphasis on ensuring the program was simple-to-use and had a user-friendly interface so designers or students, with whom have had little or no prior experience using non-linear packages, could easily understand and use the program. As such, the program was developed using Excel spreadsheets as they offer complete transparency, such that the user can easily examine and understand how the program works, while also being able to easily further develop or expand the capabilities of the program to suit their respective needs.

Many recent studies have shown it is possible to model the cyclic nonlinear force-displacement behavior of RC wall specimens in various programs that result in very good correlation with experimental test data (Hoult *et al.* 2018, Kolozvari *et al.* 2015a, Kolozvari *et al*. 2015b, Kolozvari *et al*. 2019a, Kolozvari *et al*. 2019b, Lu and Henry 2017). These studies however, have predicted the nonlinear behaviour using complex finite element packages, which are somewhat ill-suited to 'everyday' design office scenarios due to their inherent complexities and large amounts of computational resources required. Whereas the primary objective of WHAM is for it to be a simplified and transparent alternative to these other high-end modelling approaches.

WHAM is a fibre-element analysis program, which determines the moment-curvature response of a section using non-linear stress-strain material models for both concrete and reinforcement and a simplified tension stiffening model developed by the authors. The program then determines the force-displacement response by assuming an equivalent plastic hinge at the base of the wall and a linear curvature profile up the height of the wall (i.e., Eqs (1) to (6)). The plastic hinge model adopted in WHAM is the Priestley, Calvi and Kowalsky (2007) model. However, the user has the ability to easily input their own plastic hinge model or simply enter a specific plastic hinge length on case-by-case basis. An idealised force-displacement response is presented in Fig. 1.

*Corresponding author, Ph.D.
E-mail: scott@menegon.com.au

ISSN: 1598-8198 (Print), 1598-818X (Online)

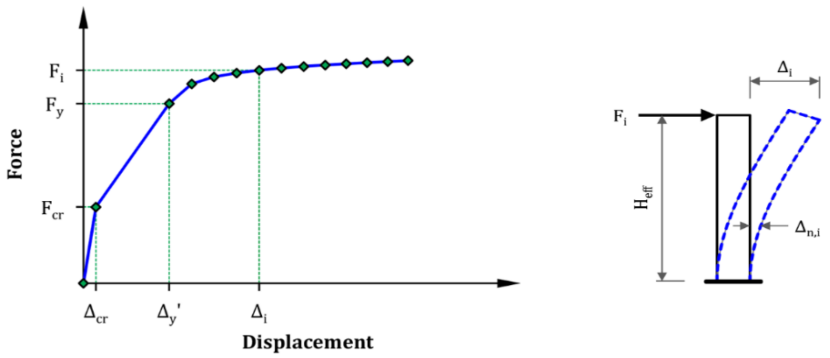

Fig. 1 Idealised force-displacement response

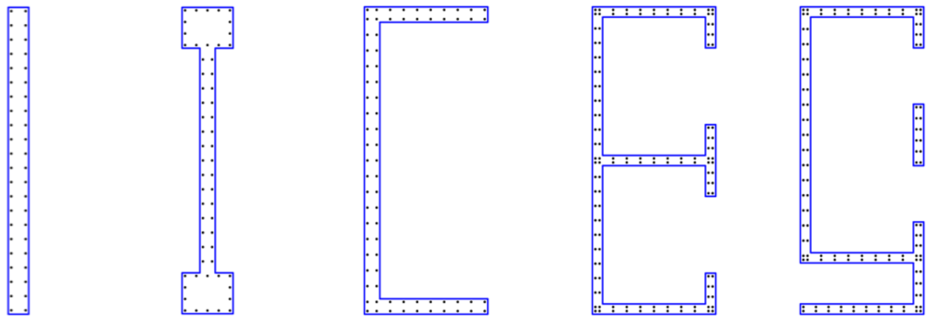

(a) rectangular (b) flanged wall (c) 'C' section (d) bundled box (e) geometric

Fig. 2 Various types of wall sections the program can accommodate.

Cracking:

$$\Delta_{cr} = \frac{\phi_{cr} H_{eff}^2}{3} \quad (1)$$

$$F_{cr} = \frac{M_{cr}}{H_{eff}} \quad (2)$$

Point of first yield:

$$\Delta'_y = \frac{\phi'_y H_{eff}^2}{3} \quad (3)$$

$$F_y = \frac{M_y}{H_{eff}} \quad (4)$$

The i-th point after first yield:

$$\Delta_i = \Delta'_y \left(\frac{M_i}{M_y}\right) + \left[\phi_i - \phi'_y \left(\frac{M_i}{M_y}\right)\right] L_p \left[H_{eff} - \left(\frac{L_p}{2} - L_{sp}\right)\right] \quad (5)$$

$$F_i = \frac{M_i}{H_{eff}} \quad (6)$$

Where: ϕ_{cr} is the cracking curvature, i.e., the point corresponding to the ultimate tensile stress of the concrete being exceeded in the extreme tensile fibre; M_{cr} is the moment capacity corresponding to the cracking curvature; H_{eff} is the effective height of the RC element; ϕ'_y is the notional yield curvature, i.e., the point corresponding to yielding of the extreme tensile reinforcing bar or the maximum compressive stress in the concrete being reached in extreme compressive fibre; M_y is the yield moment, which is the moment capacity corresponding to the notional yield curvature; ϕ_i is the curvature of the *i*-th point after yielding has occurred; M_i is the moment capacity of the *i*-th point after yielding has occurred; and L_p is the plastic hinge length, which is determined using the Priestley *et al.* (2007) model by default.

The program can handle various wall cross-sections (e.g. Fig. 2(a) to Fig. 2(e)), which can be entered manually by inputting the individual *x* and *y* nodal coordinates that make up a given section or using the section generator for a number of predetermined section geometries. The user has the option of analyzing the section as either an unconfined cross-section or a confined cross-section by entering confined regions within the section. The reinforcement in the wall can be generated automatically by entering a bar diameter and a maximum reinforcement centre-to-centre spacing or simply just a desired reinforcement ratio. The automatic reinforcement function can also be disabled, allowing the user to input each individual reinforcing bar using the *x* and *y* coordinates of each respective bar. Further, the automatic and manual functions can also be used together.

The user can also select whether the axial load on the cross-section is applied 'uniformly' through the cross-section's centroid or at a specific location, e.g., a particular outside edge of a building core that could be located on the perimeter of a floorplate. After the user has entered the required input parameters, the program determines the non-linear moment-curvature response of the cross-section using a fibre element analysis procedure written using a Visual Basic for Applications (VBA) macro. The overall broad framework of the program was initially based on the methodology presented by Lam *et al.* (2011).

The program has various built-functions to assist designers with different design tasks, such as: determining the effective stiffness (i.e., I_{eff}) of an RC section; assessing serviceability stress levels of a cross-section by

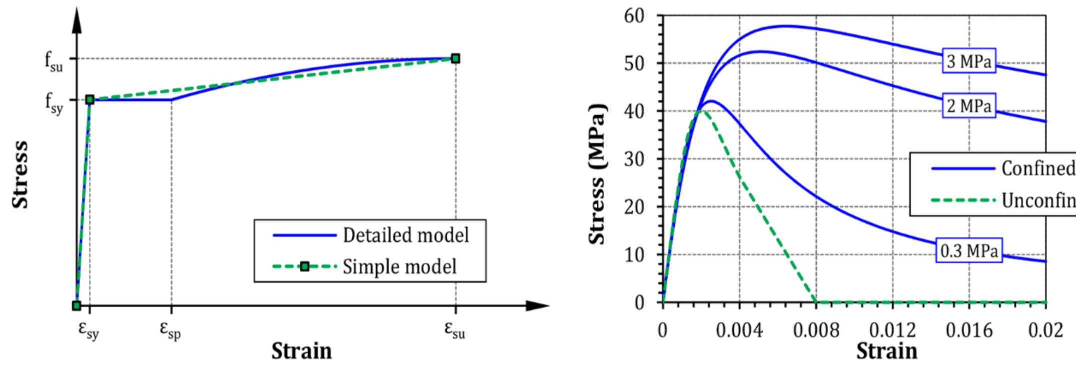

(a) reinforcement models (b) concrete model (Mander *et al.* 1988)

Fig. 3 Predefined non-linear stress-strain material models in WHAM

calculating reinforcement tensile stresses for a given applied bending moment; calculating design forces for precast wall and building core connections by assessing non-linear longitudinal shear forces at a given location in the cross-section for a given applied bending moment; and determining 'codified' interaction diagrams (i.e., axial force vs. moment capacity) for the cross-section in accordance with the Australian Standard for concrete structures, AS 3600 (Standards Australia 2018). The program also has comment boxes throughout with recommend input values and advice to assist users in an effort to make the program more user-friendly and transparent. Additional information about the user interface of the program, including example screen shots of the actual interface, is provided in the Appendix to this paper.

The primary purpose of WHAM is to predict the backbone non-linear force-displacement response of an RC wall or building core. As such, some of the more complicated failure mechanisms observed under cyclic lateral loading of RC walls, such as out-of-plane buckling instabilities (Dashti *et al.* 2017, Haro *et al.* 2019, Rosso *et al.* 2016) or local bar buckling failures (Minafo 2018, Tripathi *et al.* 2019), cannot be predicted. Alternatively, models such as Chai and Elayer (1999) can be used to calculate maximum tensile strains the wall can undergo before failure mechanisms of this nature develop. This calculated maximum tensile strain can then be entered into the program as one of the 'failure criteria' to terminate the backbone response.

2. Material models and tension stiffening model

2.1 Material models

The program allows the user to select a predefined reinforcement and concrete stress-strain material model or manually enter stress-strain curves for each respective material. The predefined reinforcement models include a simple bilinear model with a linear strain hardening region and a more detailed model that has a yield plateau region and non-linear strain hardening region. The simple model consists of two stages. The first stage is the elastic response stage that consists of a straight line from the origin with a slope of E_s (i.e., the elastic modulus of the reinforcement) up until the yield stress of the bar is reached. The second is the inelastic response stage that consists of a second straight line from the yield point to the point corresponding to the ultimate strain (i.e., uniform elongation, ε_{su}) and ultimate stress.

The detailed model consists of three stages. The first stage is the elastic response stage and is the same as the bilinear model. The second is the yield plateau region that consists of a horizontal line (i.e., constant stress) from the yield point to the yield plateau point (i.e., ε_{sp}). The third stage is the inelastic response stage that consists of a parabolic curve from the yield plateau point to the point corresponding to the ultimate strain and ultimate stress. The slope of the parabolic curve at the ultimate point is equal to zero. Both the simple and detailed models are shown in Fig. 3(a).

The predefined concrete models include the confined and unconfined Mander *et al.* (1988) and Karthik and Mander (2011) models. The Mander *et al.* (1988) model is a widely cited stress-strain model for concrete, which has been shown to provide very good correlation with experimental testing, as presented later in Section 4. However, the Mander *et al.* (1988) model was developed primarily for normal strength concrete (i.e., $f_c' \leq 50$ MPa) and as such, the Karthik and Mander (2011) model has also been included for cross-sections with high strength concrete.

It is also being recommended for 'limited ductile' or 'nominally ductile' walls that the confined Mander *et al.* (1988) model with a nominal 0.3 MPa lateral confining pressure be used for the core region of the wall, if: the horizontal reinforcement spacing is approximately equal to the thickness of the wall and lapped '*U*' bars, hooked bars or closed ligatures are specified at the end regions of the wall, as shown in Fig. 4; and the maximum compressive stresses occur at the base of the wall. The nominal 0.3 MPa lateral confining pressure provides minimal strength increase to the concrete, however it greatly increases the relative magnitude of the compressive strains on the descending 'softening' branch of the stress-strain curve, as shown in Fig. 3.

It was observed while experimentally validating the program that by allowing this nominal amount of

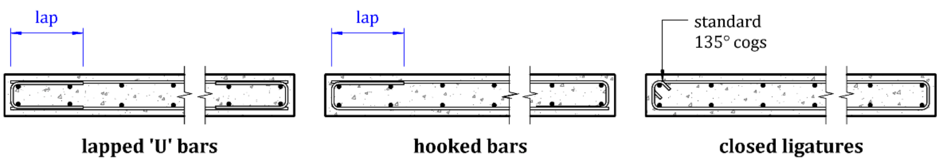

Fig. 4 Typical 'limited ductile' or 'nominally ductile' horizontal reinforcement detailing in walls

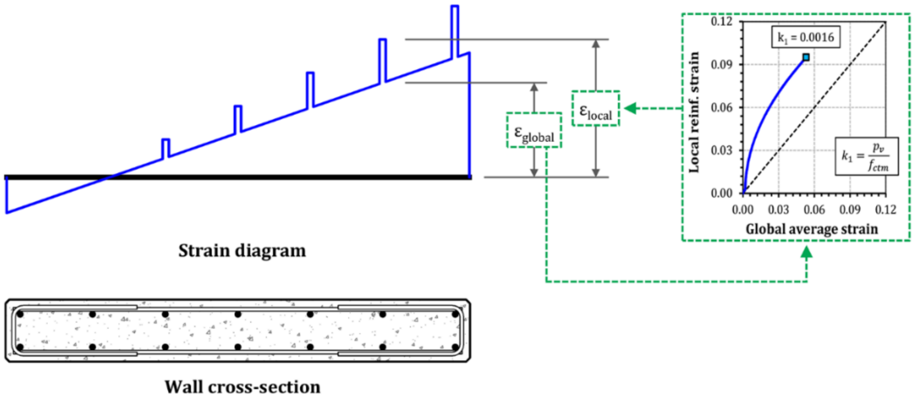

Fig. 5 Tension stiffening model implementation in WHAM

confinement to the core region of the wall in the limited ductile specimens, the resulting larger strains in the softening branch of the stress-strain curve, resulted in a much better match between the theoretical back-bone curve predicted by the program and the experimental test data in the post-peak softening region of the response. It is believed that the vertical bars at the base of the wall cantilevering out of the foundation and the varying strain/curvature gradient with a maximum compressive strain at the base of the wall (i.e., foundation) provide this nominal level of confinement. It has been pointed out by Priestley *et al*. (2007) that the "maximum compressive strains almost always occur adjacent to a supporting member (e.g., a foundation beam for a concrete column or wall), which provide an additional restraint against initiation of spalling", which translates to nominal confinement in the post-peak softening region of the concrete's stress-strain response. For comparison, well detailed walls with ductile end region confinement steel requirements would normally have a lateral confining pressure around 2 to 3 MPa in many scenarios, which results in a significant increase in compressive stress and post-peak 'softening' behavior in the stress-strain curvature, as shown in Fig. 3, which has confined stress-strain curves for lateral confining pressures of 0.3, 2 and 3 MPa.

2.2 Tension stiffening model

The program allows for tension stiffening using an experimentally validated tension stiffening model developed by the authors (Menegon 2018). While other tension stiffening models exist in literature (e.g., Patel *et al.* (2016) or Lee *et al*. (2019)), the model developed by the authors was adopted for its ease of implementation into the modelling procedure. The author's model was validated against 17 boundary element prism specimens presented in Menegon *et al*. (2019), which were designed to represent the end region of a limited ductile RC wall detailed in accordance with the Australian Standard for concrete structures, AS 3600 (Standards Australia 2018). The model allows a local reinforcement tension strain to be 'converted' to a global average tension strain of the concrete section surrounding the reinforcement. The ratio between the global and local strain is largely dependent on the crack spacing, the percentage of vertical reinforcement in the section and the tensile and bond strength of the concrete.

This tension stiffening model allows the fibre element analysis procedure to 'balance the stress block' of the RC cross-section and find equilibrium using section curvatures corresponding to global average strains of the concrete section while simultaneously using local reinforcement tensile strains and corresponding local reinforcement tensile stresses. Or put more simply, the tension strain at each reinforcing bar is increased from the average global strain to a local reinforcement strain using the tension stiffening model's average global strain to local reinforcement strain relationship. This procedure is illustrated in Fig. 5. The tension stiffening model in WHAM can be easily turned off or on with a simple input prior to undertaking the moment-curvature analysis. Tension stiffening of concrete affects walls with low percentages of vertical reinforcement significantly more compared to walls with higher percentages of vertical reinforcement. Essentially, the higher the percentage of vertical reinforcement, the more closely spaced the horizontal cracks at the tension end of the wall will be, which results in a smaller difference between average tension strains in the concrete and local tension strains in the reinforcement.

Tension stiffening is typically more important to consider in lightly reinforced specimens. An example presented in Menegon (2018) showed that the effective (i.e., cracked) moment of inertia for a wall with 0.5% vertical reinforcement ratio increased by a factor of 1.44 when tension stiffening was considered, whereas an equivalent wall with a 2.0% vertical reinforcement ratio had an

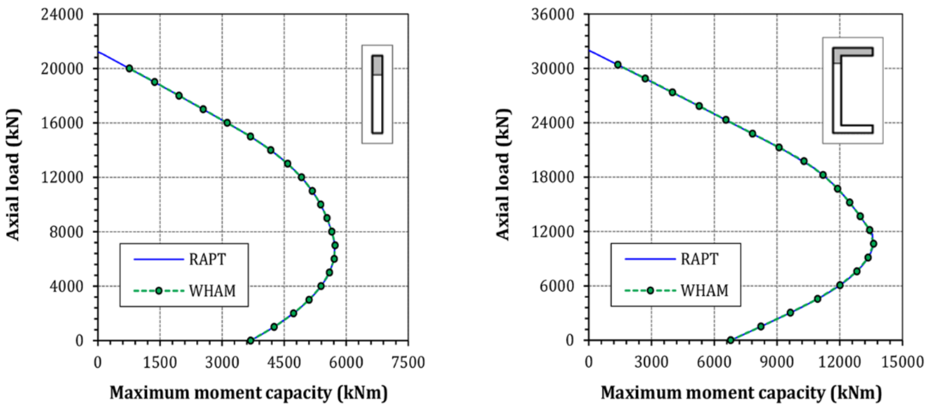

(a) rectangular wall cross-section (b) core wall cross-section

Fig. 6 Results of theoretical validation with RAPT

increase of just 1.08 to its effective moment of inertia.

3. Theorectical validation

Two approaches were adopted for validating the program. The first approach was a theoretical validation, which was being used to confirm that both the general coding and fibre element analysis engine worked and was written correctly. The theoretical approach was performed by comparing the moment-curvature results obtained from WHAM against the results from two independent software packages for two different wall cross sections. The second approach was an experimental validation, which was being using to confirm that the overall process resulted in back-bone force-displacement curves that correlated well with experimentally tested laboratory specimens of RC walls.

The theoretical validation was performed using two different software packages. The first was the commercial software package RAPT (Prestressed Concrete Design Consultants Pty Ltd 2007), which is a widely used structural analysis package for analysing conventional reinforced, prestressed and post-tensioned elements. The second was an analysis package called Response-2000 (Bentz 2000a), which is a sectional analysis program developed by researchers at the University of Toronto and is available for download free-of-charge online. The validation was performed on two different wall sections. The first was a rectangular wall section that was 2 m long and 250 mm thick with 24 mm diameter reinforcing bars on each face. The second was a core wall section that was 2.2 m long, had 1 m wide flanges, wall thicknesses of 200 mm and 20 mm diameter reinforcing bars on each face of the section. Both walls were assumed to be constructed using 40 MPa concrete.

3.1 RAPT validation

RAPT is a commercial software package that can be used to calculate the interaction diagram (i.e., axial load vs. moment capacity) of rectangular, non-rectangular and circular wall or column sections. RAPT is primarily a force-based structural design tool and as such, it calculates the maximum capacity of elements in accordance with a desired concrete standard or code, which includes AS 3600 (Standards Australia 2018), NZS 3101 (Standards New Zealand 2006), ACI 318 (American Concrete Institute 2014) or Eurocode 2 (European Committee for Standardization (CEN) 2004). This means RAPT uses characteristic material strengths and idealised material stress-strain models, as opposed to non-linear material models that represent the actual in-situ material behaviour. The primary differences between RAPT and WHAM is that RAPT is developed primarily for calculating the *characteristic* maximum capacity (i.e., strength) of an RC section in accordance with relevant standard or code. Whereas WHAM provides insight into the *actual* non-linear behavior of the section, which includes the non-linear moment-curvature response, strain distributions and non-linear deformations, in addition calculating the maximum capacity (i.e., strength) of the section.

RAPT adopts a perfectly elastic-plastic reinforcement stress-strain curve, which ignores any strain hardening of the reinforcement. The program also adopts a simplified concrete stress-strain curve, which uses a parabolic curve, with an initial slope equal to the young's modulus of the concrete, until it reaches a maximum and then constant compressive strength of $0.85f_c'$ at a compressive strain denoted ε_{co}. The manual stress-strain input in WHAM was used to enter respective material models matching those used in RAPT.

Each wall section was analysed in WHAM for incrementally increasing axial load values and the maximum moment capacity for each respective axial load was recorded to construct an interaction diagram for each wall section. The integration diagrams determined from WHAM were then overlaid on the respective RAPT interaction diagrams, as presented in Fig. 6, where it is shown that very good correlation between the two programs was achieved. The corresponding curvatures and neutral axis depths for each maximum moment calculated in WHAM also correlated very well to the RAPT values, with the same level of accuracy to what is shown in Fig. 6. This shows the general fibre element analysis engine written for WHAM correctly calculates the moment-curvature response for various RC wall sections.

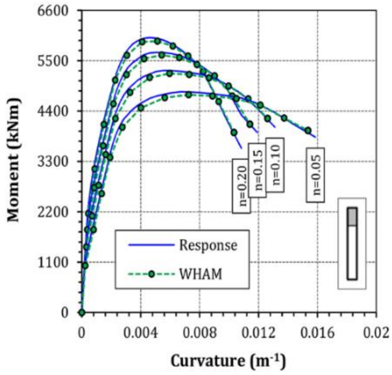

(a) rectangular wall cross-section with tension stiffening

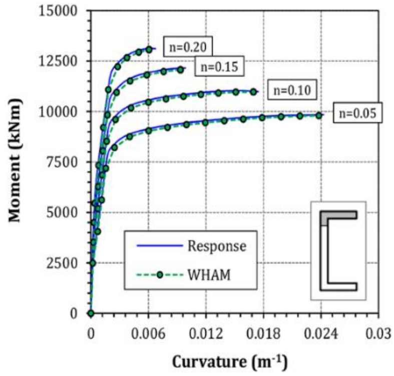

(b) core wall cross-section with tension stiffening

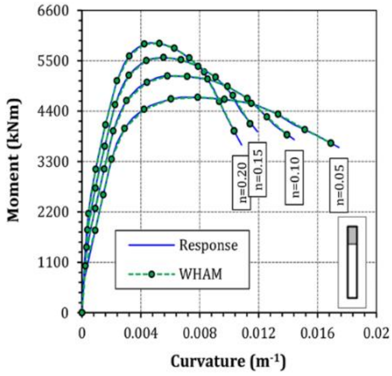

(c) rectangular wall cross-section with no tension stiffening

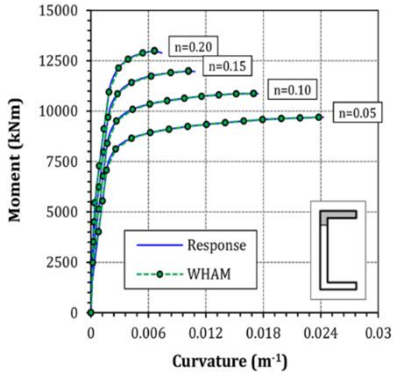

(d) core wall cross-section with no tension stiffening

Fig. 7 Results of theoretical validation with Response-2000

3.2 Response-2000 validation

Response-2000 is a sectional analysis program developed by researchers at the University of Toronto and is capable of calculating the moment-curvature response of conventional reinforced and prestressed RC elements. At their essence, Response-2000 and WHAM have a very similar functionality. The predominant difference however is the simple-to-use nature and transparent and 'open-source' aspects of WHAM, which allow it to be easily manipulated and modified by the user to suit their own respective needs. Further, this allows it to be very easily adapted for specific design scenarios or used to undertake parametric studies.

The moment-curvature response of the rectangular wall and core wall sections discussed previously were determined using Response-2000 for axial load ratios of 5%, 10%, 15% and 20%. The response was calculated using the Mander *et al.* (1988) model concrete stress-strain relationship and the detailed reinforcement stress-strain relationship discussed previously. The moment-curvature response was similarly then calculated using WHAM and compared with the results of Response-2000 (i.e., Fig. Fig. 7(a) and 7(b)).

It can be seen in Fig. 7(a) and 7(b) that Response-2000 and WHAM result in slightly different moment-curvature responses. This, is due to the tension stiffening approach adopted by each respective program. Response-2000 adopts the tension stiffening approach proposed by Bentz (2000b),

Table 1 Summary of test specimens used to experimentally validate the analysis program.

Specimen	Reference	Shear-span ratio†	Axial load ratio‡	Vert. reinf. Ratio§
S01	Menegon *et al.* (2017)*	6.5	0.065	0.018
S02		6.5	0.077	0.014
C3	Lu *et al.* (2017)	6.0	0.035	0.005
C6		4.0	0.035	0.005
WSH1	Dazio *et al.* (2009)	2.3	0.051	0.013
WSH2		2.3	0.057	0.013
WSH3		2.3	0.058	0.015
WSH4		2.3	0.057	0.015
WSH5		2.3	0.128	0.007
WSH6		2.3	0.108	0.015
A20-P10-S38	Tran and Wallace (2015)	2.0	0.073	0.032
A20-P10-S38		2.0	0.073	0.071
RW1	Thomsen and Wallace (2004)	3.1	0.100	0.023
RW2		3.1	0.070	0.023
TW1		3.1	0.090	0.014–0.023
TW2		3.1	0.075	0.014–0.015

*Additional information on this experimental program is also presented in Menegon (2018).

†Shear-span ratio equals $M^*/(V^*L_w)$, which for a 1-DOF system equals H_w/L_w (i.e., the aspect ratio).

‡Axial load ratio is equal to the applied axial load divided by the product of the concrete strength multiplied by the gross cross-sectional area of the wall, i.e., $N^*/(f_{cm}A_g)$.

§The vertical reinforcement ratio for the specimens with concentrated regions of reinforcement refers to the end region (i.e., boundary element) ratio, whereas otherwise it refers to the average vertical reinforcement ratio of the entire cross-section.

whereas WHAM uses the procedure discussed previously. When tension stiffening is turned off in each respective program the moment-curvature results correlate very well to each other (refer Fig. 7(c) and 7(d)), providing good validation that the fibre element analysis engine written for WHAM works as intended and produces good results.

4. Experimental validation

The experimental validation was performed by comparing the back-bone force-displacement response calculated using WHAM against the cyclic force-displacement response of 16 test specimens from literature. The 16 test specimens were tested as part of five different test programs conducted internationally and consisted of both rectangular and non-rectangular wall sections. The 16 test specimens had a wide range of parameters, which included shear-span ratios that varied from 2.0 to 6.5, axial load ratios varying from 0.035 to 0.128 and vertical reinforcement ratios varying from 0.005 to 0.071. A summary of the 16 test specimens is presented in Table 1 and the cross sections of each test specimen from the literature is presented in Fig. 8 and 9. For further specimen details the reader is directed to the relevant test program cited in Table 1.

The analysis was performed using the unconfined Mander *et al*. (1988) model for the concrete in the cover regions and similarly, the confined Mander *et al*. (1988) model for the concrete in the core region of the wall. The reinforcement model that best matched the stress-strain properties of the reinforcement in the respective test

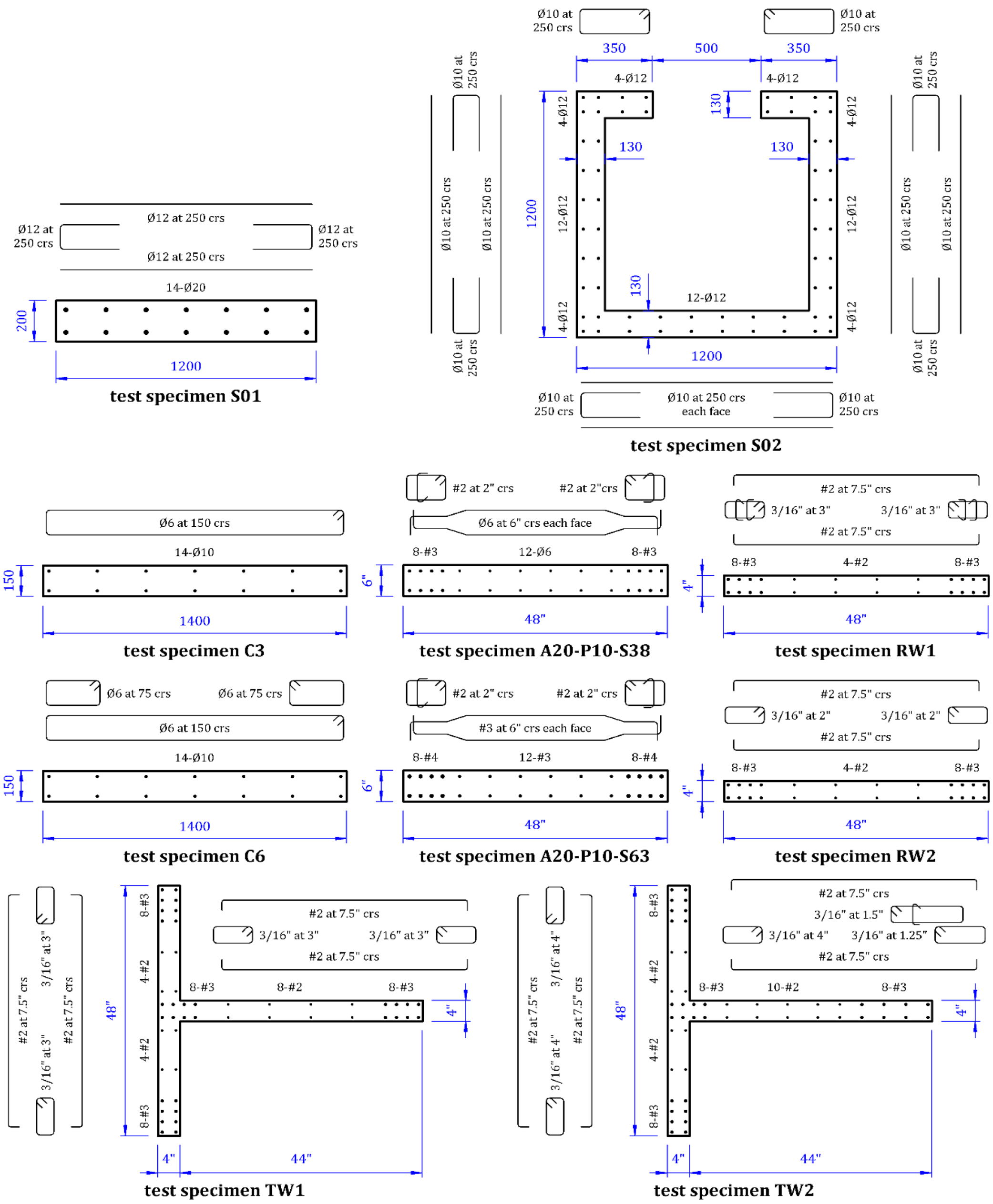

Fig. 8 Wall specimen cross-sections used to experimentally validate WHAM (1 of 2)

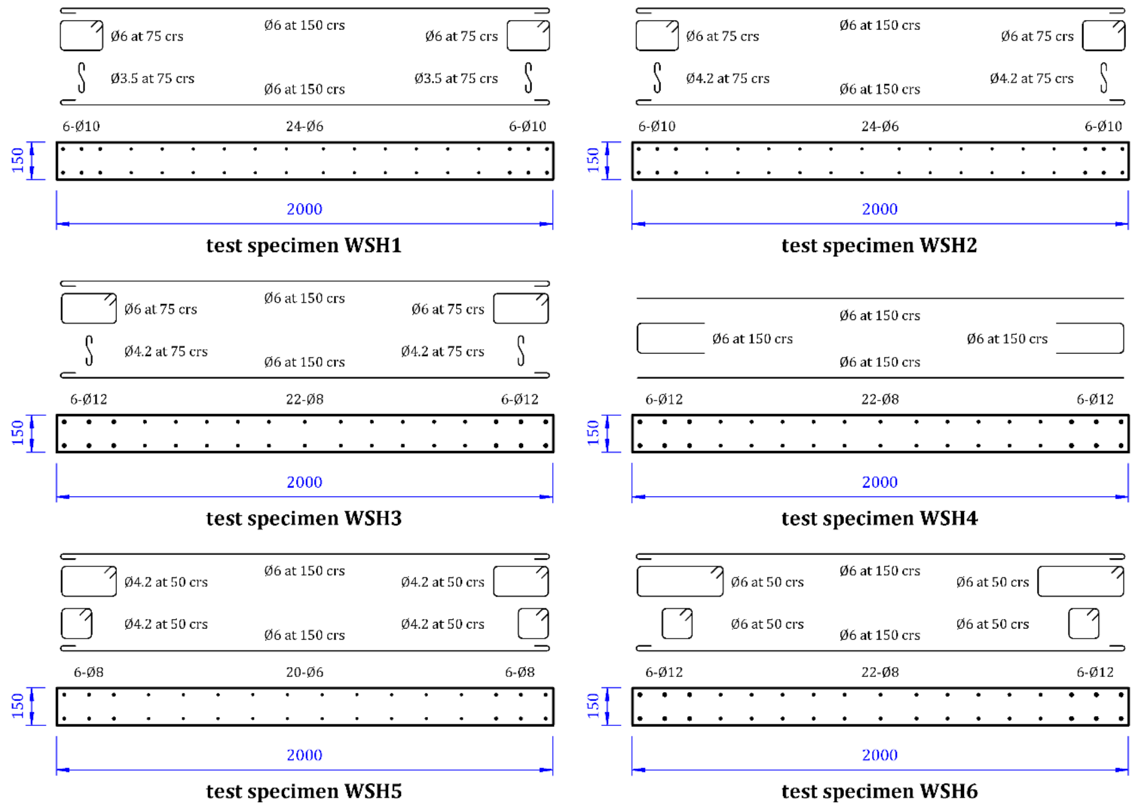

Fig. 9 Wall specimen cross-sections used to experimentally validate WHAM (2 of 2)

program was adopted, for example, specimens that used coiled reinforcement, which does not have a yield plateau region, the detailed model with no yield plateau was adopted, whereas specimens that only the yield stress, ultimate stress and ultimate strain were given for each specimen in the study, the simple bilinear model was adopted.

For the limited ductile test specimens, i.e., S01, S02, C3 and WSH4, the confined Mander *et al.* (1988) model with a nominal lateral confining pressure of 0.3 MPa was adopted (as discussed previously). Whereas, for the remaining 12 specimens, the lateral confining pressure was calculated based on the reinforcement detailing (refer Figs. 8 and 9) and the formulas given in Mander *et al.* (1988). The results of the force-displacement analysis using WHAM and the associated comparison to the corresponding test specimen is presented in Fig. 10 and Fig. 12. The correlation between the results of WHAM and the test specimens from each respective test program (as summarised in Table 1) are discussed in the following five sub-sections and then followed by a brief summary discussing the overall accuracy and performance of WHAM.

The default plastic hinge model adopted in WHAM is the Priestley *et al.* (2007) model, as discussed in the first section of this paper. This plastic hinge model was selected because it was found to result in the best correlation with the results of the experimental test specimens presented in this section, which cover a wide range of different wall parameters (refer Table 1). Multiple other models were also investigated, including the models proposed by Bohl and Adebar (2011), Hoult *et al.* (2018), Kazaz (2013) and Thomsen and Wallace (2004), however the Priestley *et al.* (2007) model was found to have the best correlation with the experimental results. However, it should be noted that the user has the ability to easily input their own plastic hinge model into WHAM, as such, using the Priestley *et al.* (2007) model is optional.

4.1 Menegon et al. (2017)–specimens S01 and S02

Test specimens S01 and S02 were tested as 'panel specimens' where only the bottom portion of an equivalent taller wall is tested. Under this test setup an in-plane moment coupled to the in-plane lateral force resistance of the specimen is applied to simulate the bending moment and shear force response of the equivalent bottom section of the taller wall. As such, WHAM was used to calculate the force-displacement response of the specimen itself (Fig. 10(a) and Fig. 10(d), respectively) and the equivalent taller specimen (Fig. 10(b) and Fig. 10(e), respectively).

The back-bone force-displacement response of S01 determined using WHAM correlates quite well with the equivalent 1-DOF response (i.e., Fig. 10(b)). The test specimen response (i.e., Fig. 10(a)) also correlated quite well, however WHAM seemed to slightly under predict the yield displacement and the subsequent inelastic displacements by a small margin.

The displacement response of S02 correlated somewhat well with the equivalent 1-DOF response (i.e., Fig. 10(e)), however the strength capacity predicted by WHAM was higher than what was observed during the test. Menegon (2018) reports that during the construction of S02 poor

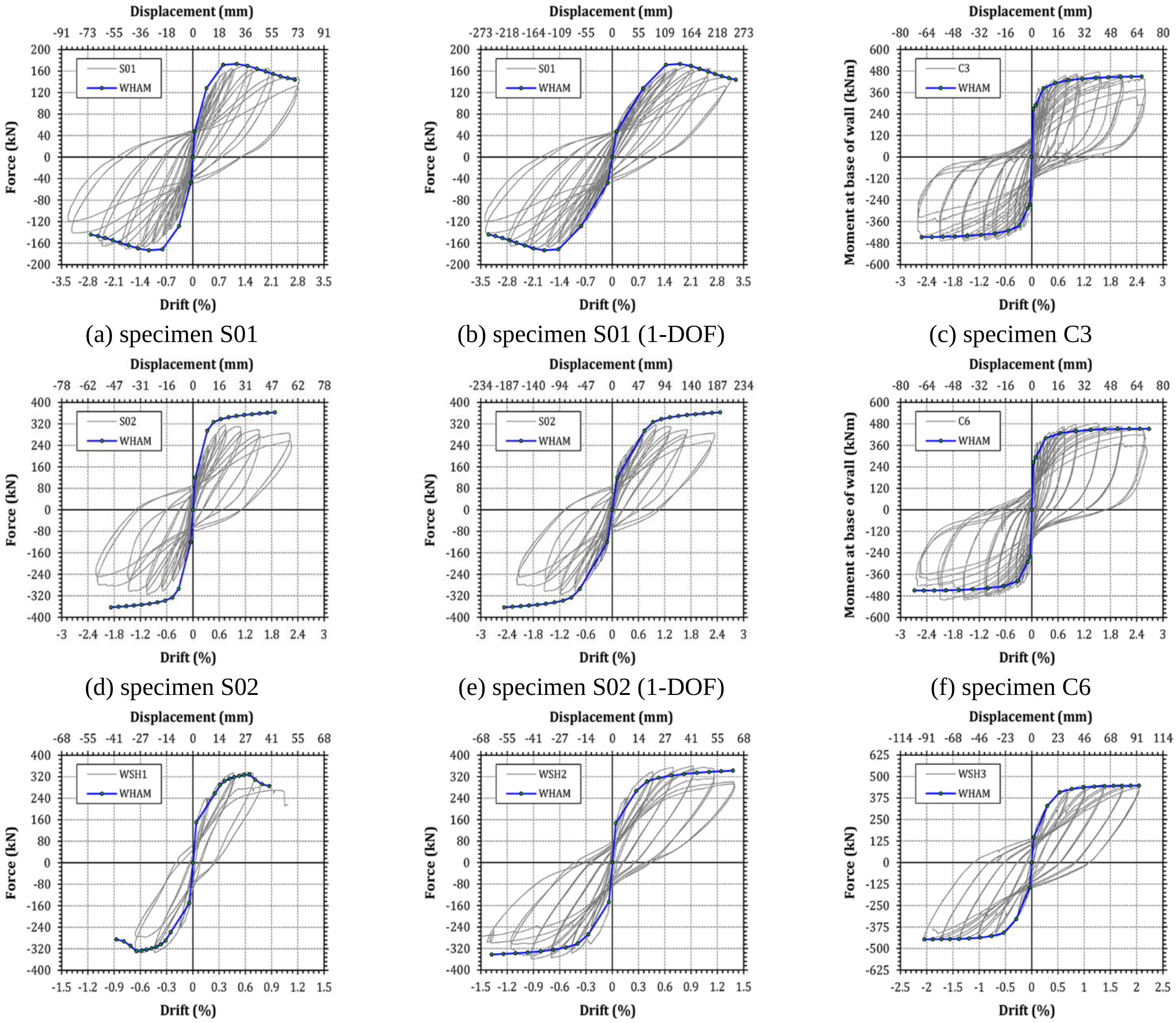

(a) specimen S01 (b) specimen S01 (1-DOF) (c) specimen C3

(d) specimen S02 (e) specimen S02 (1-DOF) (f) specimen C6

(g) specimen WSH1 (h) specimen WSH2 (i) specimen WSH3

Fig. 10 Results of experimental validation of WHAM (1 of 2)

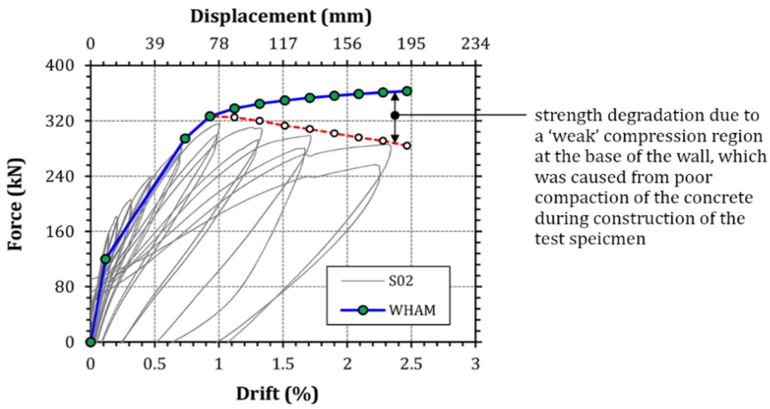

Fig. 11 Strength degradation in test specimen S02

vibration of the concrete occurred around the base of the specimen, which required some patch fixing after the formwork was stripped. This poor vibration and compaction meant that the concrete at the base of the wall in the maximum moment region was locally weakened, with reduced bond strength capacity to the reinforcement, which then resulted in a gradual 10% loss in lateral capacity from about 1.0% to 2.3% lateral drift (as highlighted in Fig. 11).

If the specimen was constructed with satisfactory concrete compaction in this region there would likely not

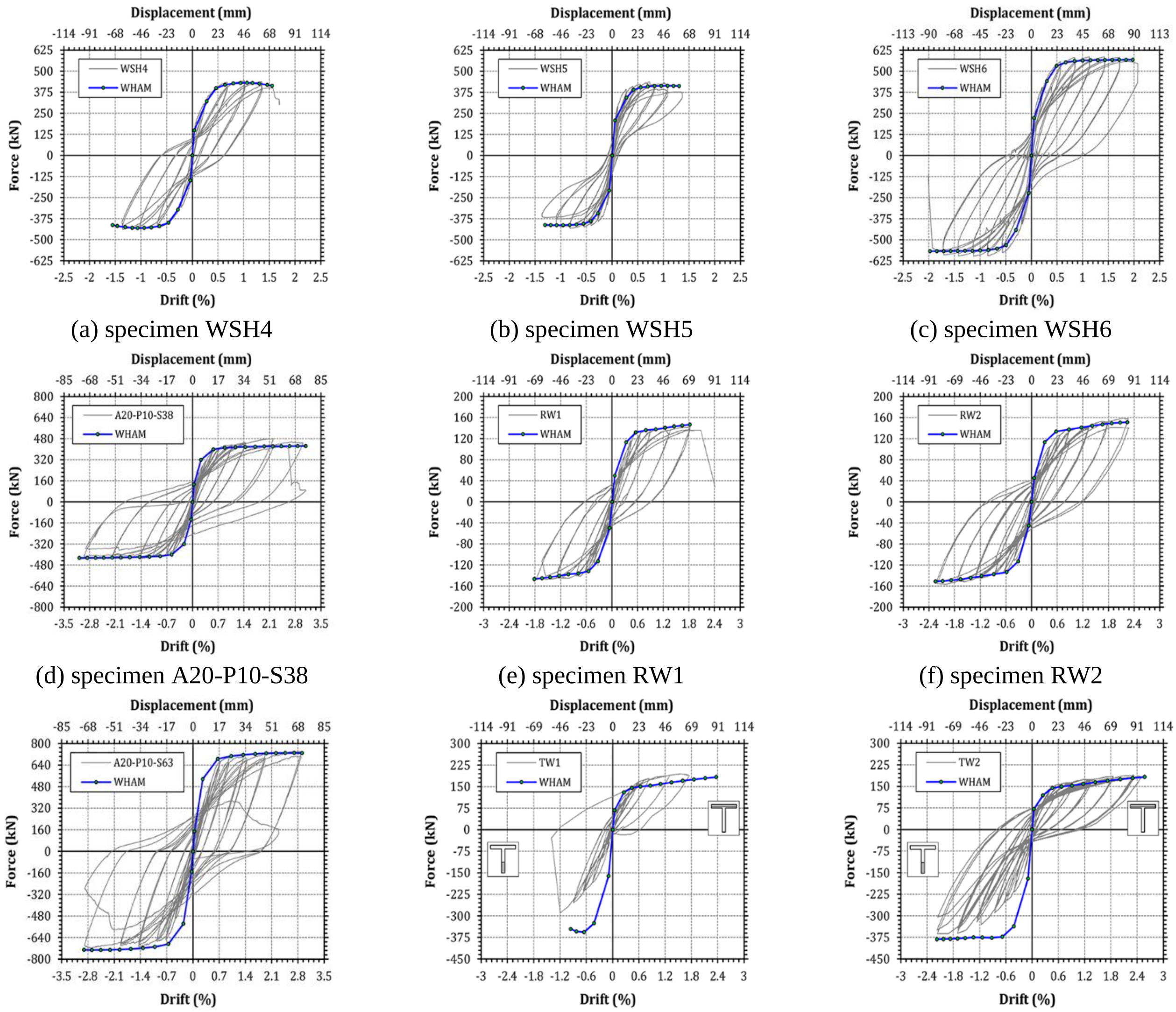

(a) specimen WSH4 (b) specimen WSH5 (c) specimen WSH6
(d) specimen A20-P10-S38 (e) specimen RW1 (f) specimen RW2
(g) specimen A20-P10-S63 (h) specimen TW1 (i) specimen TW2

Fig. 12 Results of experimental validation of WHAM (2 of 2)

have been this 10-15% strength decrease (across the lateral drift region highlighted in Fig. 11), which then would have resulted in quite a good match between WHAM and the response of S02. WHAM however, seemed to under predict the test specimen displacements (i.e., storey displacements), with good correlation not being observed (i.e., Fig. 10(d)).

The plastic hinge equations proposed by Priestley *et al*. (2007), which form the basis of WHAM (i.e., Eqs. (1) to (6)), were developed for walls without lap splices where the inelastic curvature is solely concentrated at the base of the wall (i.e., in the typical plastic hinge region). Test specimens S01 and S02 were constructed with lap splices at the base of the wall in the plastic hinge region, which resulted in atypical inelastic curvature and strain distributions. Interestingly though, despite these different curvature and inelastic strain distributions, Eqs. (1) to (6) still seemed to predict the displacements fairly well.

4.2 Lu et al. (2017)–specimens C3 and C6

Fairly good correlation was observed between test specimens C3 and C6 and the program WHAM, i.e., Fig. 10(c) and Fig. 10(f), respectively. WHAM slightly underpredicted the maximum moment capacity of each specimen, particularly specimen C6 in the negative loading direction. The program was not able to capture the strength drop in C6 that occurred around -2% lateral drift, which was due to fracturing of the two extreme tensile face reinforcing bars. Lu *et al*. (2017) reported that these two bars buckled on the previous reversed positive load cycle of +1.5% lateral drift, which means the fracturing of these two bars and ensuing strength drop could have been a result of a low cycle fatigue induced fracturing of the reinforcement, as opposed to the ultimate strain (determined from monotonic tensile tests) being reached. WHAM can obviously predict the latter; however, the former scenario is outside the scope and ability of the program.

4.3 Dazio et al. (2009)–specimens WSH1 and WSH6

Very good correlation was generally observed between test specimens WSH1 to WSH6 and the program, as

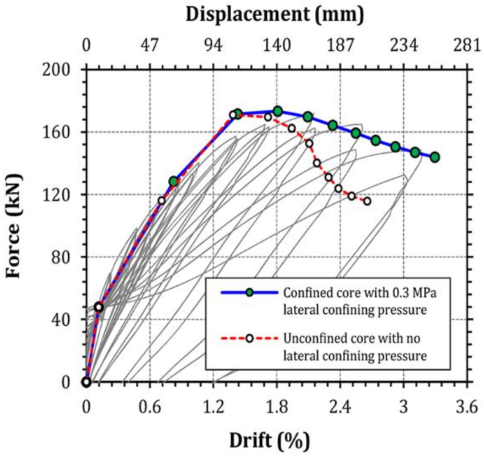

(a) specimen S01 (1-DOF)

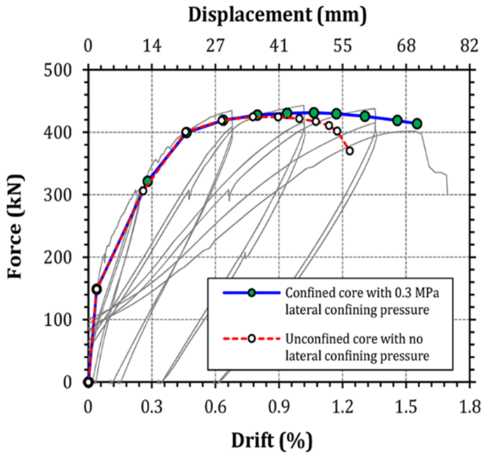

(b) specimen WSH4

Fig. 13 Modelling limited ductile walls with nominal lateral confinement pressure to core

presented in Fig. 10(g) to Fig. 10(i) for WSH1 to WSH3 and Fig. 12(a) to Fig. 12(c) for WSH4 to WSH6, respectively. The behaviour of specimen WSH1 was predicted very well, including the fracturing of the vertical reinforcement that occurred between lateral drift values of 0.6% to 0.9%. WSH1 was detailed using the European equivalent of D500L reinforcement in Australia (i.e., low ductility reinforcement), which is why failure of the specimen occurred at much smaller lateral drift compared to the other five specimens, i.e., WSH2 to WSH6.

Specimens WSH3, WSH4 and WSH6 all had very good correlation between WHAM and the test data, particularly WSH4, which was a limited ductile specimen. This very good correlation, in addition to the predicted responses of the other limited ductile rectangular specimens (i.e., S01 and C3), supports the proposed adopted nominal lateral confinement pressure of 0.3 MPa for limited ductile walls, which was discussed and proposed in Section 2. This is further illustrated in Fig. 13(a) and Fig. 13(b), which shows a comparison of specimens S01 and WSH4, respectively, of how the predicted back-bone force-displacement response changes when the confined Mander *et al*. (1988) model with nominal 0.3 MPa lateral confining pressure is used for the core of the wall as opposed to using the unconfined Mander *et al*. (1988) model for the whole cross-section.

The correlation between test specimens WSH2 and WSH5 and the program was not as high as specimens WSH1, WSH3, WSH4 and WSH6, however it was still fairly good. The program did not capture the strength degradation that occurred on the last positive and negative loading increments for both specimens. The program also slightly underestimated the strength of WSH2.

4.4 Tran and Wallace (2015)–specimens A20-P10-S38 and A20-P10-S63

Fairly good correlation was observed between test specimens A20-P10-S38 (i.e., S38) and A20-P10-S63 (i.e., S63) and the program, i.e., Fig. 12(d) and Fig. 12(g), respectively. Interestingly, the program predicted the strength of S38 quite well in the negative direction, however it slightly underpredicted it in the positive direction. The strength was then predicted fairly well in both the positive and negative directions for S63.

While the general back-bone force-displacement behaviour was predicted generally quite well for both specimens, the yield displacement was underpredicted for both specimens, however particularly in specimen S63, which results in a significantly different effective stiffness between the actual response and the program.

4.5 Thomsen and Wallace (2004)–specimens RW1, RW2, TW1 and TW2

Quite good correlation was observed between the rectangular test specimens RW1 and RW2 and the program, i.e., Fig. 12(e) and Fig. 12(f), respectively. The yield displacement in specimen RW2 was slightly underestimated in the positive direction, however in the negative direction, the yield displacement was estimated fairly accurately. Otherwise, the force-displacement response was estimated fairly accurately for both specimens.

Test specimens TW1 and TW2 had relatively quite poor correlation compared to RW1 and RW2 (refer Fig. 12(h) and Fig. 12(i), respectively). The general force-displacement response of TW2 in the positive direction (i.e., the flange in compression and the web in tension) was generally quite good, however then in the negative direction (i.e., the web in compression and the flange in tension) the strength was significantly overestimated for lateral drifts below about -2%. The strength of TW1 in the positive direction was underestimated and then overestimated in the negative direction. The poor correlation in this instance could be due to the effective flange width, which varied during the test, but in the model is considered as a constant width equal to the actual width of the flange. Further investigation is required in this instance.

4.6 Validation summary

Overall, very good correlation was observed between the experimental test data of the rectangular walls and the theoretical predictions of the test program. This included test specimens with a wide range of shear-span ratios, axial load ratios and vertical reinforcements ratios. This shows the program can quite confidently predict the back-bone force-displacement behaviour of rectangular walls and particularly, limited ductile rectangular walls, which are of particular importance to this research project.

A limited number of specimens were used to validate the programs ability to predict the back-bone force-displacement behaviour of non-rectangular walls. For the most part, the correlation was not as strong as the rectangular walls. Further research and development is recommended for non-rectangular walls, which may require the development and implementation of a different plastic hinge model specifically for non-rectangular walls of various cross sections. In the interim, with respect to non-rectangular wall sections, the program should be limited to performing only non-linear moment-curvature analyses.

5. Conclusions

This paper has outlined the development of a simple, user-friendly and transparent analysis program for predicting the back-bone force-displacement behaviour of slender (i.e., flexure-controlled) RC walls and building cores. The program is called WHAM and is written using Microsoft Excel spreadsheets and is available free-of-charge. The program is intended to be used as an educational tool for structural designers, researchers or students. The program was validated using both theoretical and experimental approaches. The theoretical validation of WHAM was conducted by performing moment-curvature analyses on walls with different cross sections and axial load ratios and comparing the results against a widely used commercial software package called RAPT and a sectional analysis program developed by researchers at the University of Toronto called Response-2000. Very good correlation was observed between the results from WHAM and the two independent software packages, providing strong validation that the fibre element analysis engine written for WHAM works as intended and produces good results.

The experimental validation was performed by comparing the back-bone force-displacement response calculated using WHAM against the results of 16 test specimens as reported in the literature that were tested as part of five different test programs. Very good correlation was observed between WHAM and the rectangular wall test specimens, which included a wide variation of walls with shear-span ratios ranging from 2.0 to 6.5, axial load ratios from 3.5% to 12.8% and percentages of vertical reinforcement from 0.5% to 7.1%. Only a limited number of comparisons were performed against non-rectangular wall test specimens, however the correlation was not as good for these sections.

Acknowledgments

Financial support from the Australian Research Council (ARC) Discovery Project DP140103350 entitled *Collapse Assessment of Reinforced Concrete Buildings in Regions of Lower Seismicity* is gratefully acknowledged.

References

American Concrete Institute (2014), ACI 318-14 Building Code Requirements for Structural Concrete, American Concrete Institute, Farmington Hills, MI.

Bentz, E. (2000a), Response-2000, University of Toronto, Toronto, Canada.

Bentz, E.C. (2000b), "Sectional analysis of reinforced concrete", Doctor of Philosophy Thesis, Department of Civil Engineering, University of Toronto.

Bohl, A. and Adebar, P. (2011), "Plastic hinge lengths in high-rise concrete shear walls", *ACI Struct. J.*, **108**(2), 148-157.

Chai, Y.H. and Elayer, D.T. (1999), "Lateral stability of reinforced concrete columns under axial reversed cyclic tension and compression", *ACI Struct. J.*, **96**(5), 780-789.

Dashti, F., Dhakal, R.P. and Pampanin, S. (2017), "An experimental study on out-of-plane deformations of rectangular structural walls subject to in-plane loading", *Proceedings of the 16th World Conference on Earthquake Engineering*, Santiago, Chile, January.

Dazio, A., Beyer, K. and Bachmann, H. (2009), "Quasi-static cyclic tests and plastic hinge analysis of RC structural walls", *Eng. Struct.*, **31**(7), 1556-1571. https://doi.org/10.1016/j.engstruct.2009.02.018.

European Committee for Standardization (Cen) (2004), Eurocode 2: Design of Concrete Structures - Part 1-1: General Rules and Rules for Buildings, European Committee for Standardization (CEN), Brussels, Belgium.

Haro, A.G., Kowalsky, M. and Chai, Y.H. (2019), "Out‐of‐plane buckling instability limit state for boundary regions of special RC structural walls", *Bull. Earthq. Eng.*, **17**(9), 5159-5182. https://doi.org/10.1007/s10518-019-00667-4.

Hoult, R., Goldsworthy, H. and Lumantarna, E. (2018), "Plastic hinge length for lightly reinforced rectangular concrete walls", *J. Earthq. Eng.*, **22**(8), 1447-1478. https://doi.org/10.1080/13632469.2017.1286619.

Karthik, M.M. and Mander, J.B. (2011), "Stress-block parameters for unconfined and confined concrete based on a unified stress-strain model", *J. Struct. Eng.*, **137**(2), 270-273. https://doi.org/10.1061/(ASCE)ST.1943-541X.0000294.

Kazaz, I. (2013), "Analytical study on plastic hinge length of structural walls", *J. Struct. Eng.*, **139**(11), 1938-1950. https://doi.org/10.1061/(ASCE)ST.1943-541X.0000770.

Kolozvari, K., Biscombe, L., Dashti, F., Dhakal, R.P., Gogus, A., Gullu, M.F., ... & Shegay, A. (2019b), "State-of-the-art in nonlinear finite element modeling of isolated planar reinforced concrete walls", *Eng. Struct.*, **194**, 46-65. https://doi.org/10.1016/j.engstruct.2019.04.097.

Kolozvari, K., Kalbasi, K., Orakcal, K., Massone, L.M. and Wallace, J. (2019a), "Shear-flexure-interaction models for planar and flanged reinforced concrete walls", *Bull. Earthq. Eng.*, 17(12), 6391-6417. https://doi.org/10.1007/s10518-019-00658-5.

Kolozvari, K., Orakcal, K. and Wallace, J.W. (2015a), "Modeling of cyclic shear-flexure interaction in reinforced concrete structural walls. I: Theory", *J. Struct. Eng.*, **141**(5), 4014135. https://doi.org/10.1061/(ASCE)ST.1943-541X.0001059.

Kolozvari, K., Tran, T.A., Orakcal, K. and Wallace, J.W. (2015b), "Modeling of cyclic shear-flexure interaction in reinforced concrete structural walls. II: Experimental validation", *J. Struct. Eng.*, **141**(5), 4014135.

https://doi.org/10.1061/(ASCE)ST.1943-541X.0001083.
Lam, N., Wilson, J. and Lumantarna, E. (2011), "Force-deformation behaviour modelling of cracking reinforced concrete by EXCEL spreadsheets", *Comput. Concrete*, **8**(1), 43-57. https://doi.org/10.12989/cac.2011.8.1.043.
Lee, J.H., Jung, C.Y., Woo, T.R. and Cheung, J.H. (2019), "Post-yielding tension stiffening of reinforced concrete members using an image analysis method with a consideration of steel ratios", *Adv. Concrete Constr.*, **7**(2), 117-126. https://doi.org/10.12989/acc.2019.7.2.117.
Lu, Y. and Henry, R.S. (2017), "Numerical modelling of reinforced concrete walls with minimum vertical reinforcement", *Eng Struct.*, **143**, 330-345. https://doi.org/10.1016/j.engstruct.2017.02.043.
Lu, Y., Henry, R.S., Gultom, R. and Ma, Q.T. (2017), "Cyclic testing of reinforced concrete walls with distributed minimum vertical reinforcement", *J. Struct. Eng.*, **143**(5), 04016225. https://doi.org/10.1061/(ASCE)ST.1943-541X.0001723.
Mander, J.B., Priestley, M.J.N. and Park, R. (1988), "Theoretical stress-strain model for confined concrete", *J. Struct. Eng.*, ASCE, **114**(8), 1827-1849. https://doi.org/10.1061/(ASCE)0733-9445(1988)114:8(1804).
Menegon, S.J. (2018), "Displacement behaviour of reinforced concrete walls in regions of lower seismicity", Doctor of Philosophy Thesis, Department of Civil and Construction Engineering, Swinburne University of Technology.
Menegon, S.J. (2019), *WHAM: a User-friendly and Transparent Non-linear Analysis Program for RC Walls and Building Cores*, https://downloads.menegon.com.au/1/20190901.
Menegon, S.J., Wilson, J.L., Lam, N.T.K. and Gad, E.F. (2017), "Experimental testing of reinforced concrete walls in regions of lower seismicity", *Bull. NZ Soc. Earthq. Eng.*, **50**(4), 494-503. https://doi.org/10.5459/bnzsee.50.4.494-503.
Menegon, S.J., Wilson, J.L., Lam, N.T.K. and Gad, E.F. (2019), "Experimental testing of nonductile RC wall boundary elements", *ACI Struct. J.*, **116**(6), 213-225, https://doi.org/10.14359/51718008.
Minafo, G. (2018), "Local buckling of reinforcing steel bars in RC members under compression forces", *Comput. Concrete*, **22**(6), 527-538. https://doi.org/10.12989/cac.2018.22.6.527.
Patel, K.A., Chaudhary, S. and Nagpal, A.K. (2016), "A tension stiffening model for analysis of RC flexural members under service load", *Comput. Concrete*, **17**(1), 29-51. https://doi.org/10.12989/cac.2016.17.1.029.
Prestressed Concrete Design Consultants Pty Ltd. (2007), RAPT, Prestressed Concrete Design Consultants Pty Ltd., Alexandra Headland, Australia.
Priestley, M.J.N., Calvi, G.M. and Kowalsky, M.J. (2007), *Displacement-Based Seismic Design of Structures*, IUSS Press, Pavia, Italy.
Rosso, A., Almeida, J.P. and Beyer, K. (2016), "Stability of thin reinforced concrete walls under cyclic loads: state-of-the-art and new experimental findings", *Bull. Earthq. Eng.*, **14**(2), 455-484. https://doi.org/10.1007/s10518-015-9827-x.
Standards Australia (2018), AS 3600:2018 Concrete Structures, Standards Australia Limited, Sydney, NSW.
Standards New Zealand (2006), NZS 3101:Part 1:2006 Concrete Structures Standard Part 1 - The Design of Concrete Structures, Standards New Zealand, Wellington.
Thomsen, J.H. and Wallace, J.W. (2004), "Displacement-based design of slender reinforced concrete structural walls-Experimental verification", *J. Struct. Eng.*, **130**(4), 618-630. https://doi.org/10.1061/(ASCE)0733-9445(2004)130:4(618).
Tran, T.A. and Wallace, J.W. (2015), "Cyclic testing of moderate-aspect-ratio reinforced concrete structural walls", *ACI Struct. J.*, **112**(6), 653-665.
Tripathi, M., Dhakal, R.P. and Dashti, F. (2019), "Bar buckling in ductile RC walls with different boundary zone detailing: Experimental investigation", *Eng. Struct.*, **198**, 109544. https://doi.org/10.1016/j.engstruct.2019.109544.

SF

Appendix: WHAM user interface

This appendix provides a more detailed description of WHAM's user interface. As discussed in the paper, WHAM was developed and written using Microsoft Excel spreadsheets. The analysis and computation work performed within the program is undertaken using Visual Basic for Applications (VBA) subroutines. The program is split across a series of worksheets. The initial input sheet allows the user to choose from one of a series of 'standard' cross-sections (e.g., a T-section, where the user just has to then enter the wall length, flange wall width and the web and flange wall thicknesses) or alternatively, the user can enter a custom cross-section by inputting the specific *x* and y co-ordinates of each corner point of the section. A screen shot of this initial input page is shown in Fig. 14. There is then a second input page where the cross-sections reinforcement can be generated (either automatically based on a maximum bar spacing or alternatively by entering the x and y co-ordinates of each bar) and confined regions within the cross-section can be specified (as shown in Fig. 15). After the RC section details have been entered, the cross-section can be analysed. There are three analysis sheets: the first sheet is the nonlinear moment-curvature analysis and results page (as shown in Fig. 16); the second sheet is the nonlinear back-bone force-displacement response and results page; and the third sheet is a 'code' analysis, which calculates an AS 3600 code compliant interaction diagram (i.e., axial-force vs. moment diagram).

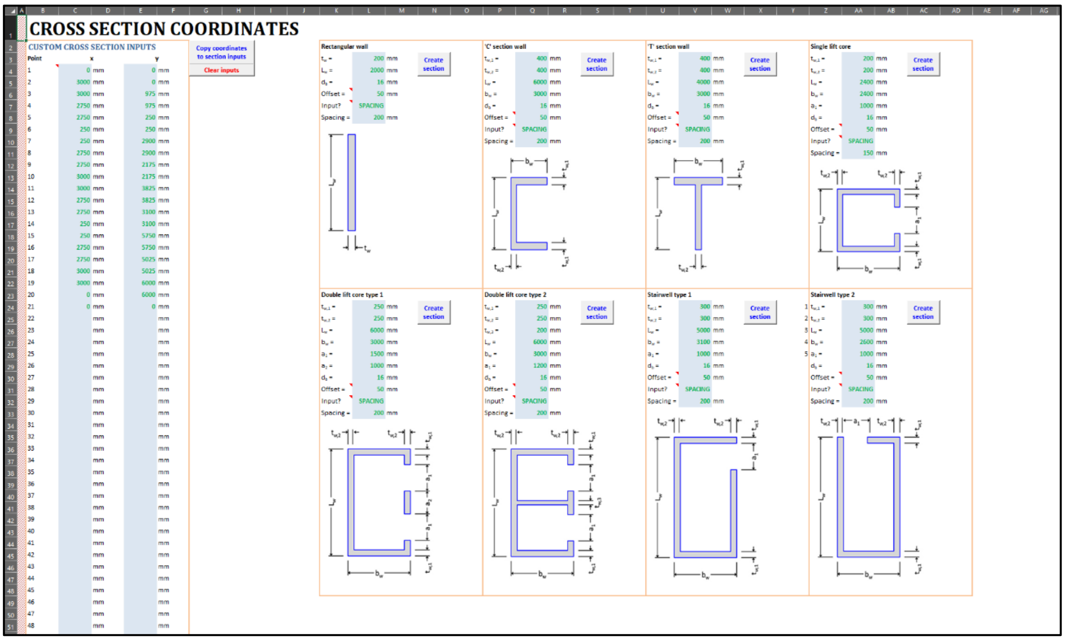

Fig. 14 WHAM user interface: typical cross section input page

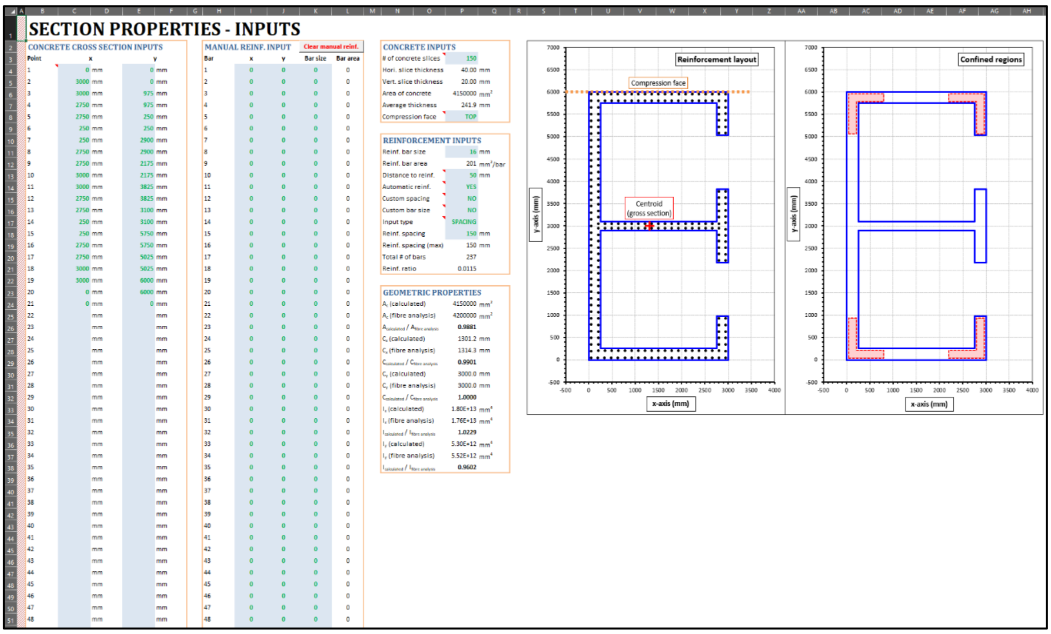

Fig. 15 WHAM user interface: cross-section details page

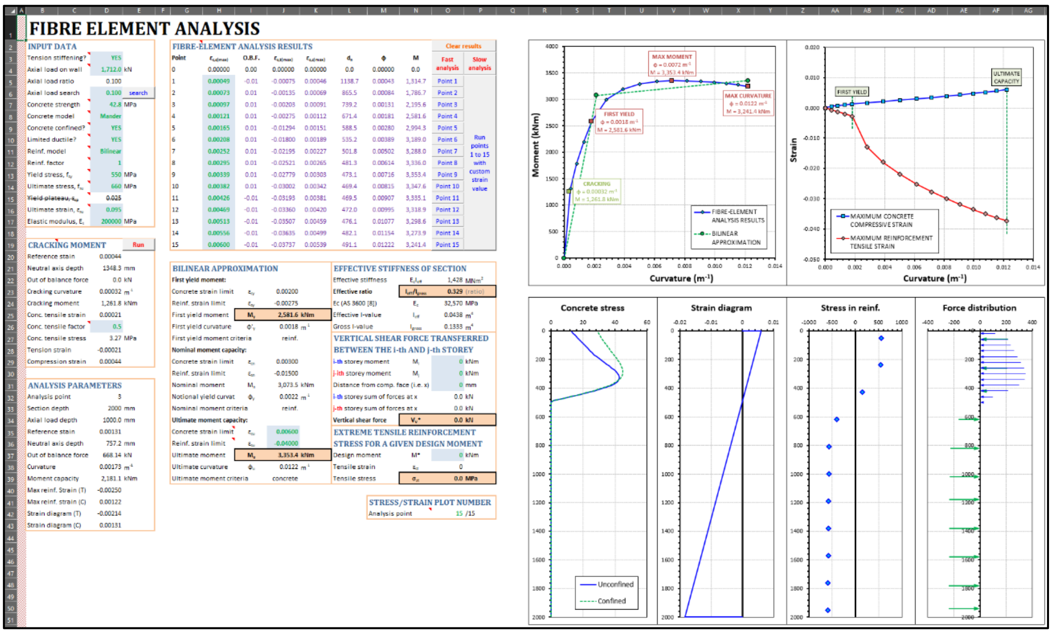

Fig. 16 WHAM user interface: moment-curvature analysis output page